FEBS Letters 580 (2006) 2577–2583

Enzymatic activity of the SARS coronavirus main proteinase dimer

Vito Graziano, William J. McGrath, Ann Marie DeGruccio, John J. Dunn, Walter F. Mangel*

Biology Department, Brookhaven National Laboratory, Upton, NY 11973, USA

Received 20 December 2005; revised 23 March 2006; accepted 3 April 2006

Available online 21 April 2006

Edited by Hans-Dieter Klenk

Abstract **The enzymatic activity of the SARS coronavirus main proteinase dimer was characterized by a sensitive, quantitative assay. The new, fluorogenic substrate, (Ala-Arg-Leu-Gln-NH)$_2$-Rhodamine, contained a severe acute respiratory syndrome coronavirus (SARS CoV) main proteinase consensus cleavage sequence and Rhodamine 110, one of the most detectable compounds known, as the reporter group. The gene for the enzyme was cloned in the absence of purification tags, expressed in *Escherichia coli* and the enzyme purified. Enzyme activity from the SARS CoV main proteinase dimer could readily be detected at low pM concentrations. The enzyme exhibited a high K_m, and is unusually sensitive to ionic strength and reducing agents.**

Keywords: Antiviral agents; Fluorogenic substrate; High throughput screening; Proteinase; Rhodamine; SARS

1. Introduction

Severe acute respiratory syndrome (SARS) has been implicated in more than 8000 cases and 900 related deaths since 2003. A coronavirus was identified as the major cause of SARS [1,2]. The genome of the SARS coronavirus (SARS CoV), a positive-stranded RNA virus, has been sequenced [3,4]. The SARS coronavirus replicase gene contains two overlapping translation products, polyprotein 1a (~450 kDa) and polyprotein 1ab (~750 kDa). The polyproteins are cleaved by virus-coded proteinases, one of which is the 3C-like or SARS CoV main proteinase, a cysteine proteinase with a chymotrypsin-like fold [5]. Prevention of the proteolytic processing of coronavirus replicase polyproteins inhibits the production of infectious virus particles [6], and for this reason the SARS CoV main proteinase is an attractive target for antiviral agents. However, before potential inhibitors can be screened, a sensitive and quantitative assay for enzyme activity must be developed.

Amino acid derivatives of Rhodamine 110 have been shown to be extremely sensitive, specific and selective substrates for proteinases [7–11]. Bis-substituted substrates are virtually nonfluorescent, because the fluorophore is in the lactone state. Upon cleavage by an endoproteinase of one of the two amide bonds adjacent to the Rhodamine moiety, the Rhodamine moiety in the resultant mono-substituted product switches to the quinone state exhibiting a high degree of conjugation; concomitant with this is a massive increase in fluorescence intensity. Rhodamine-based substrates have been used to assay caspases in vitro [12] and in vivo; trypsin, plasmin and thrombin [8]; leucine aminopeptidase and dipeptidyl aminopeptidase in solution [13] and on the cell surface [14]; cathepsin K in vivo expressed in CHO cells [15]; elastase [16]; and the adenovirus proteinase [10,11].

Here we describe the synthesis and purification of a highly sensitive fluorogenic substrate for the SARS CoV main proteinase, (Ala-Arg-Leu-Gln-NH)$_2$-Rhodamine, and the use of this substrate in the development of a sensitive, and quantitative assay for the enzyme. The amino acid sequence Ala-Arg-Leu-Gln is similar to sequences recognized by the SARS CoV main proteinase at cleavage sites in the replicase polyprotein [17,18]; cleavage occurs after Gln. We also cloned the gene for the SARS CoV main proteinase, expressed the gene in *Escherichia coli* without purification tags, and purified the enzyme. With this substrate, an extremely sensitive, quantitative assay was developed for measuring SARS CoV main proteinase activity. This assay has not only been useful in characterizing the enzyme but also should be useful in the detection of inhibitors via high-throughput screening that are potential antiviral agents.

2. Materials and methods

2.1. Materials and methods in Supplementary material

Described in detail in the Supplementary material are: The synthesis and purification of the fluorogenic substrate (Ala-Arg-Leu-Gln-NH)$_2$-Rhodamine, cloning of the SARS CoV main proteinase, expression and purification of the SARS CoV main proteinase, and conversion of the primary data in an assay to pmol substrate hydrolyzed per unit time.

2.2. Assays of the SARS CoV main proteinase

SARS CoV main proteinase in a solution of 25 mM Tris–HCl (pH 8) was incubated for 5 min at room temperature or at 37 °C. Then, (Ala-Arg-Leu-Gln-NH)$_2$-Rhodamine was added, and the increase with time in absorbance at 496 nm or in fluorescence at 523 nm was measured. Continuous fluorescence intensity measurements were made with an ISS model PC-1 (ISS, Champaign, IL) photon counting spectrofluorometer using a 300-W xenon arc lamp and 17 ampere lamp current. The excitation and emission wavelengths were set to 492 and 523 nm, respectively, with 8 nm excitation and emission slits. Fluorescence intensity assays were also performed on a TECAN ULTRA 384 plate reader using Greiner black flat bottom 384-well non-treated

*Corresponding author. Fax: +1 631 344 3407.
E-mail address: mangel@bnl.gov (W.F. Mangel).

Abbreviations: DTT, dithiothreitol; SARS CoV, severe acute respiratory syndrome coronavirus

0014-5793/$32.00
doi:10.1016/j.febslet.2006.04.004

microplates. The reaction volume was 100 μL. The excitation and emission wavelength filters used were 485 and 535 nm, respectively. Before each experiment, the gain and Z-position were optimized using a reaction containing the maximal amount of fluorescence that could be generated in the experiment. The integration time was 40 μs with 10 lamp flashes per measurement. The time-dependent increase in fluorescence intensity was monitored, on average, every 9 s depending on the number of wells being read.

3. Results

3.1. Synthesis and purification of the fluorogenic substrate (Ala-Arg-Leu-Gln-NH)$_2$-Rhodamine

(Cbz-Gln-NH)$_2$-Rhodamine was synthesized by incubating the *p*-nitrophenyl ester of *N*-α-CBZ-L-glutamine with Rhodamine110. The product of the reaction was purified by precipitation with water. After deblocking with HBr in acetic acid, (Cbz-Leu-Gln-NH)$_2$-Rhodamine was synthesized by activating the carboxylic acid group of Cbz-L-leucine with 1-ethyl-3-(3-dimethylaminopropyl)carbodiimide hydrochloride and incubation with (Gln-NH)$_2$-Rhodamine. This process was repeated for the addition of Arg and then Ala. The final product (Ala-Arg-Leu-Gln-NH)$_2$-Rhodamine was purified by flash chromatography and HPLC.

The structures of the bis-amide substrate (Ala-Arg-Leu-Gln-NH)$_2$-Rhodamine, its hydrolysis product (Ala-Arg-Leu-Gln-NH)-Rhodamine, and Rhodamine110 along with their absorption and emission spectra are shown in Fig. 1. The bis-amide substrate does not absorb in the visible range as the Rhodamine moiety is in the lactone state. Upon cleavage of (Ala-Arg-Leu-Gln-NH)$_2$-Rhodamine by the SARS CoV main proteinase, the mono-amide product (Ala-Arg-Leu-Gln-NH)-Rhodamine is formed. The mono-substituted product absorbs around 490 nm, because the Rhodamine-moiety is in the quinone state. Ala-Arg-Leu-Gln-NH-Rhodamine exhibits two, overlapping absorbance peaks with maxima at 469 and 492 nm, whereas Rhodamine 110 has a single absorbance peak at 496 nm. One interpretation for the origin of the split peak in the mono-substituted product is: The bis-substituted substrate is not symmetrical; cleavage of one bond on (Ala-Arg-Leu-Gln-NH)$_2$-Rhodamine may give rise to a species that absorbs slightly differently than if cleavage occurred at the other amide bond.

3.2. Cloning, expression and purification of the SARS CoV main proteinase

The SARS CoV main proteinase was cloned from viral mRNA in virus-infected Vero cells via RT-PCR. The bound-

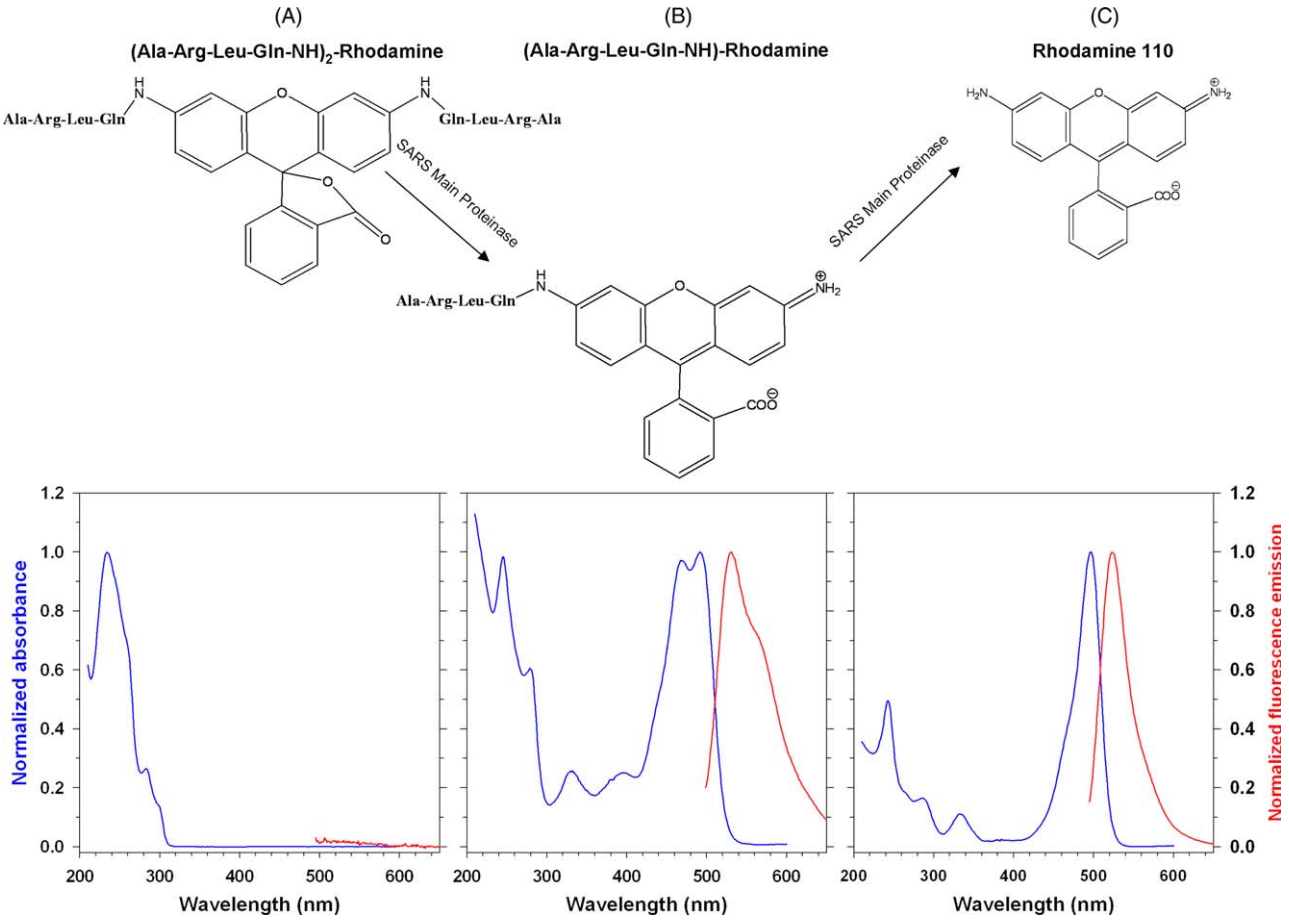

Fig. 1. Chemical structure of the fluorogenic substrate (Ala-Arg-Leu-Gln-NH)$_2$-Rhodamine (A), its hydrolysis product (Ala-Arg-Leu-Gln-NH)-Rhodamine (B), and Rhodmaine110 (C), with their corresponding normalized absorbance spectra. The absorption spectrum in (A) indicates (Ala-Arg-Leu-Gln-NH)$_2$-Rhodamine does not absorb between 460 and 500 nm, therefore the Rhodamine moiety is drawn in the lactone state. Upon hydrolysis by the SARS CoV main proteinase, the product, in (B), absorbs strongly between 460 and 500 nm, therefore the Rhodamine moiety is drawn in the quinone state.

aries of the gene were 3241Lys-Gln3240 [19]. The gene was ligated into pET11d plasmid and the resultant plasmid electroporated into TOP10 cells for propagation. Finally, the pET11d-SARS plasmid was transformed into electrocompetent *E. coli* BL21(DE3) cells. For expression, the BL21(DE3) cells were grown overnight in autoinduction medium [20]. A large amount of the enzyme appeared in the supernatant after centrifugation of the cell lysate, Fig. 2. The soluble proteinase in the supernatant flowed through a strong cation column connected in series to a strong anion column. The last step in the purification procedure was to apply that flow through to a different strong anion column. The weakly bound enzyme eluted at a low salt concentration. The cell extract must be very dilute in order for the enzyme to bind to the POROS 50HQ column. At this stage, the enzyme was estimated to be greater than 98% pure. The enzyme is difficult to purify because it has a p*I* of 6.2 with a net negative charge density of only 3. Its molecular mass determined by Maldi was 33 759; this indicates that N-terminal methionine was missing.

3.3. Kinetics of hydrolysis of (Ala-Arg-Leu-Gln-NH)$_2$-Rhodamine by the SARS CoV main proteinase

Is (Ala-Arg-Leu-Gln-NH)$_2$-Rhodamine a substrate for the SARS CoV main proteinase? Four different concentrations of the SARS CoV main proteinase were incubated with 20 μM (Ala-Arg-Leu-Gln-NH)$_2$-Rhodamine and the increase in fluorescence monitored as a function of time. The results, Fig. 3, showed that (Ala-Arg-Leu-Gln-NH)$_2$-Rhodamine was indeed a substrate for the SARS CoV main proteinase. The increase in fluorescence with time was linear for at least 5 min. The rates of change in fluorescence, 12, 44, 159, and 231 pM(s)$^{-1}$ increased with increasing enzyme concentrations 125, 250, 500, and 750 nM, respectively. As a control, the SARS CoV main proteinase was incubated with the fluorogenic substrate for the adenovirus proteinase (Leu-Arg-Gly-Gly-NH)$_2$-Rhodamine [10,11]. No hydrolysis of the compound was observed (data not shown).

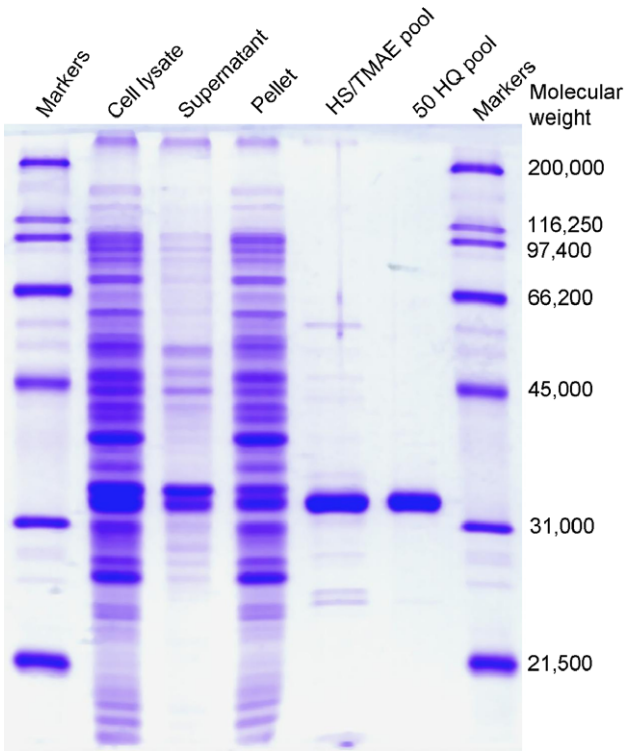

Fig. 2. Analysis of the purification of the SARS CoV main proteinase by SDS polyacrylamide gel electrophoresis. The left and right end lanes contain molecular weight markers, with the numbers shown on the right indicating the molecular weights of the markers in Da . Lane 2 contains the whole cell extract after cell lysis with lysozyme. Lanes 3 and 4 show the supernatant and pellet, respectively, after centrifugation at 30 000 × *g* for 30 min. Lane 5 contains the enzyme pool after passage through strong cation/anion columns in series. Lane 6 shows the enzyme pool after elution from a second strong anion column. The SDS–polyacrylamide gel contained 12.5% acrylamide.

3.4. Optimization of the assay conditions

The effects on enzyme activity of pH, temperature, NaCl concentration, dithiothreitol (DTT) concentration, and NP-40 concentration were ascertained in order to optimize the assay conditions, Fig. 4. The pH optimum was 8.0, Fig. 4A. The solid line is the best fit to the experimental data points using a model system with two ionizable groups with pK_a values of 6.8 and 8.7. The optimal temperature for enzyme activity was about 42 °C, Fig. 4B. Enzyme activity increased by only 37% between 25 and 37 °C. There was a dramatic decrease in enzyme activity between 42 and 47 °C. Enzyme activity was very sensitive to ionic strength, Fig. 4C. Over 80% of enzyme activity was inhibited by the presence of 100 mM NaCl. A similar sensitivity was observed with DTT, Fig. 4D. Over 80% of enzyme activity was inhibited in the presence of 2.5 mM DTT. The nonionic detergent NP-40 also inhibited enzyme activity, Fig. 4E; about 80% of enzyme activity was inhibited by the presence of 0.1% (v/v) NP-40.

3.5. Michaelis–Menten parameters

The macroscopic kinetic constants were obtained by incubating 3 μM SARS CoV main proteinase with different concentrations of (Ala-Arg-Leu-Gln-NH)$_2$-Rhodamine and measuring the increase in absorbance at 496 nm as a function

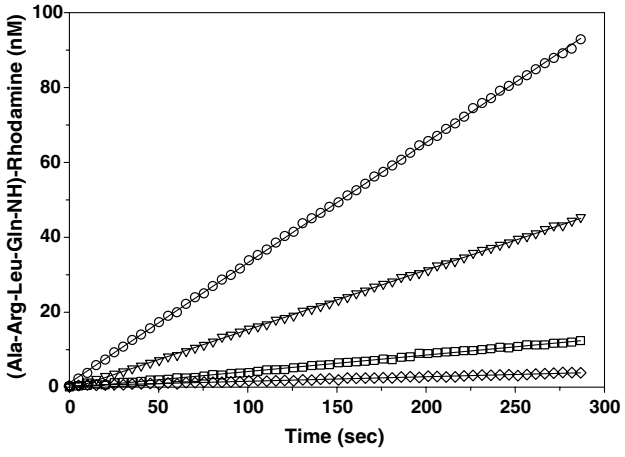

Fig. 3. Kinetics of hydrolysis of (Ala-Arg-Leu-Gln-NH)$_2$-Rhodamine by the SARS CoV main proteinase. The SARS CoV main proteinase at concentrations of (◇) 0.125 μM, (□) 0.25 μM, (▽) 0.50 μM, and (○) 0.75 μM were incubated with 20 μM (Ala-Arg-Leu-Gln-NH)$_2$-Rhodamine in 1 mL of 25 mM Tris–HCl (pH 8) and the increase in fluorescence monitored as a function of time. Conversion of arbitrary fluorescence units to nM substrate hydrolyzed was accomplished by use of a standard curve.

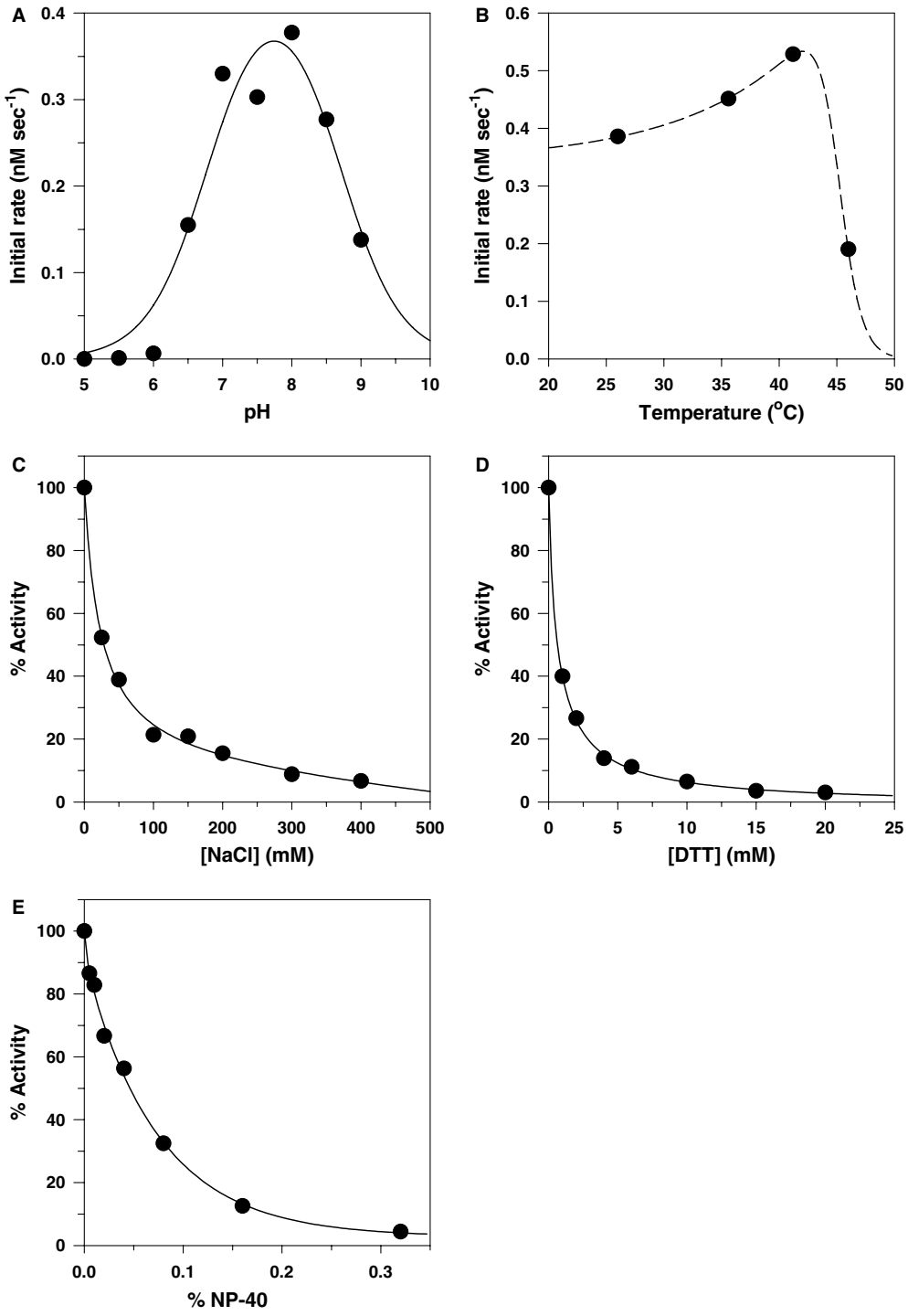

Fig. 4. Effect of pH (A), temperature (B), (NaCl) (C), dithiothreitol (D), and NP-40 (E) on the activity of the SARS CoV main proteinase. Assays were performed at 21 °C except those in (B). The reaction mixtures contained 1 μM SARS CoV main proteinase and 20 μM (Ala-Arg-Leu-Gln-$NH)_2$-Rhodamine in 1 mL 25 mM Tris–HCl (pH 8.0). Enzyme activity was monitored spectrofluorometrically. (A) Initial rates of substrate hydrolysis are plotted as a function of pH in 25 mM buffers made at the indicated pHs with sodium citrate, MES, HEPES, TRIS or CHES. The solid line is the best fit to the experimental data points using a model system with two ionizable groups. (B) Initial rates of substrate hydrolysis are plotted as a function of temperature in 25 mM Tris–HCl (pH 8) buffer. (C)–(F) The effect of increasing concentrations of NaCl, dithiothreitol or NP-40 on SARS CoV main proteinase activity were measured.

of time. The data are shown in Fig. 5, a plot of the rate of substrate hydrolysis versus the substrate concentration. The rate of substrate hydrolysis at lower substrate concentrations was proportional to the concentration of substrate. At higher concentrations of substrate, the rate of hydrolysis approached saturation. The data could be fit to the classic Michaelis–Menten hyperbola, the solid line. From this hyperbola, a K_m of 306 μM and a k_{cat} of 0.92 min^{-1} were calculated.

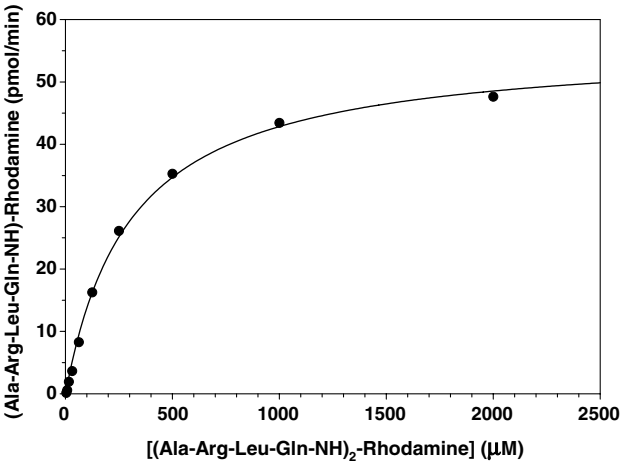

Fig. 5. Michaelis–Menten analysis of the interaction of (Ala-Arg-Leu-Gln-NH)$_2$-Rhodamine with the SARS CoV main proteinase. All reactions, in 100 μL, contained 3 μM SARS CoV main proteinase, 4% dimethylsulfoxide, 25 mM Tris–HCl (pH 8.0) and the following concentrations of substrate: 3.9, 7.8, 15.6, 31.2, 62.5, 125, 250, 500, 1000, or 2000 μM. The rate of hydrolysis was measured by following the change in absorbance at 496 nm as a function of time. The initial velocities obtained from the data are plotted versus substrate concentration. The rectangular hyperbola was drawn by fitting the data to the Michalis–Menten equation from which a K_m of 306 μM and a k_{cat} of 0.92 (min)$^{-1}$ were calculated.

3.6. Sensitivity of the assay

How sensitive is this assay for the SARS CoV main proteinase using (Ala-Arg-Leu-Gln-NH)$_2$-Rhodamine as a substrate? Decreasing concentrations of enzyme, from 325 to 1 nM, were incubated with 20 μM (Ala-Arg-Leu-Gln-NH)$_2$-Rhodamine and the increase in fluorescence at 523 nm measured as a function of time. Linear kinetics were observed (data not shown). When the rate of substrate hydrolysis was plotted versus the SARS CoV main proteinase concentration, the profile was an exponential function [Graziano et al., in preparation]. However, when the rate of substrate hydrolysis was plotted versus the dimer concentration of the SARS CoV main proteinase, the profile was a straight line through the origin, Fig. 6. The dimer concentration was calculated using a monomer–dimer equilibrium dissociation constant of 6.8 μM [Graziano et al., in preparation].

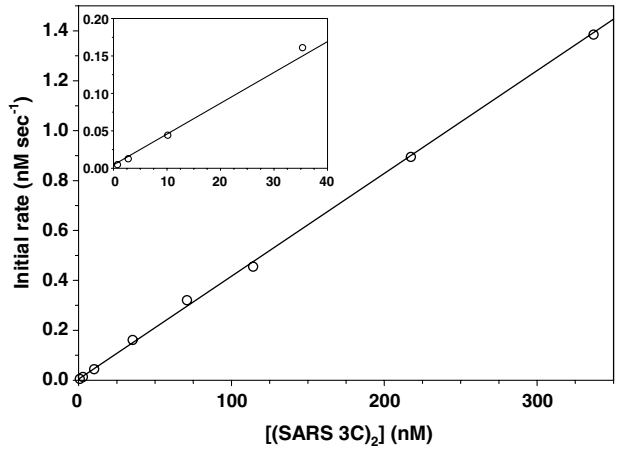

Fig. 6. Sensitivity of the SARS CoV main proteinase assay. Different concentrations of the SARS CoV main proteinase dimer, ranging from 325 nM to 1 nM, were incubated with 10 μM (Ala-Arg-Leu-Gln-NH)$_2$-Rhodamine in 25 mM Tris–HCl (pH 8.0) and the increase in fluorescence at 523 nm with time measured. The dimer concentration (SARS 3C)$_2$ was calculated based upon the monomer–dimer equilibrium dissociation constant of 6.8 μM (Graziano et al., manuscript in preparation).

4. Discussion

Compared to other assays for the SARS CoV main proteinase, the assay using (Ala-Arg-Leu-Gln-NH)$_2$-Rhodamine as the substrate is much more sensitive, by orders of magnitude. The least sensitive and most laborious assay for the SARS CoV main proteinase monitors cleavage of peptides by reverse phase HPLC [18,21,5]. A continuous, chromogenic enzyme assay has been developed using *p*-nitroanilide as the chromophore [22]. However, the extinction coefficient of paranitroanilide is 8800 M^{-1} cm^{-1}, compared to greater than 70 000 M^{-1} cm^{-1} for Rhodamine110 [7]. A fluorescence resonance energy transfer (FRET) substrate with Dabcyl and Edans as the FRET pair and a sequence of 12 amino acid residues containing a SARS CoV main proteinase preferred cleavage site has also been used in an assay for the SARS CoV main proteinase [23]. This assay is not very sensitive, because the extinction coefficient of Edans at 336 nm is 5438 M^{-1} cm^{-1}, and the quantum yield is only 0.36 [24]. The quantum yield for Rhodamine110 is greater than 0.90 [7]. Furthermore, a substrate containing FRET pairs incorporated into a peptide of 12 amino acids is very expensive.

The amino acid sequence (Ala-Arg-Leu-Gln) was chosen for the Rhodamine-based substrate for several reasons. Studies of the 11 conserved interdomain junctions cleaved on the viral polyprotein by the SARS CoV main proteinase revealed that the substrate specificity is determined by the amino acids in the P2, P1 and P1′ positions [17,18]. All 11 cleavage sites in the SARS coronavirus polyprotein have a conserved Gln in the P1 position, 8 have a Leu in the P2 position, and 9 have either Ala or Ser in the P1′ position. Peptides with other amino acids in the P2, P1, and P1′ positions are poorer substrates or are not cleaved at all. More recently, studies of 34 peptide substrates reveal that residues at positions P4 and P3 are also critical for substrate recognition and binding [25]. The P3 position likes a positively charged amino acid. The P4 position likes amino acids with high β-sheet tendency, such as Val or Thr.

Bis-substituted derivatives of Rhodamine110 are sensitive, specific and selective substrates for proteinases, a combination exhibited by no other class of synthetic substrates. They are sensitive substrates, because they are nonfluorescent, but, upon cleavage of a single amide bond become highly fluorescent, exhibiting large molar absorbance coefficients and quantum yields over a wide pH range, from pH 3 to 12. They are particularly useful in the neutral to basic pH range where the output from a xenon lamp is relatively high and where interference from most biological compounds is low. They are specific substrates whose specificity is further enhanced upon cleavage of a single amide bond, because the fluorophore undergoes conversion from the lactone to the quinone state. This process is accompanied by an increase in the de-

gree of conjugation and hence stability which leads to an enhancement of the reactivity of the susceptible bonds in the substrate. They are selective substrates because their structure mimics the amino acid sequence in the reactive site of a proteinase's natural substrate.

The bifunctionality of the bis-substituted Rhodamine-based substrates does not complicate the interpretation of kinetic data, provided that no more than 5% of the substrate is hydrolyzed during an assay. Indeed, bi-functionality may even confer certain advantages. The effective concentration of susceptible amide bonds is twice the substrate concentration. Also, the presence of two peptides per Rhodamine110 moiety may enhance the solubility of the substrate.

How do the properties of mono-substituted Rhodamine and Rhodamine110 compare to those of the highly used reporting group 7-amino-4-methylcoumarin? The relative detectabilites of different fluorophores under enzyme assay conditions [7] can be compared using a molar fluorescence coefficient, whose dimensions are relative fluorescence units per molar concentration of fluorophore. The molar fluorescence coefficient of mono-substituted Rhodamine is 4.5-fold greater than that for 7-amino-4-methylcoumarin. This difference is, in part, the result of the absorption of mono-substituted Rhodamine being 5-fold greater than that of 7-amino-4-methylcoumarin, the quantum yield for mono-substituted Rhodamine being 0.5-fold that of 7-amino-4-methylcoumarin, the efficiency of the excitation optics at 492 nm being 3-fold greater than that at 380 nm, and the efficiency of the emission optics at 523 being 0.62-fold that at 460 nm. The molar fluorescence coefficient of Rhodamine110 is 45-fold greater than that for 7-amino-4-methylcoumarin.

The Michaelis constant, K_m, of 306 μM is unusually high for a Rhodamine-based substrate. The k_{cat} was 0.92 min^{-1}. However, this is probably a reflection of the enzyme and not the substrate. Fluorescence resonance energy transfer (FRET) substrates have been used to measure the enzymatic activity of the SARS CoV main proteinase. They have yielded K_m values ranging from 404 to 16 μM [23,26–30]. With EDANS-VNSTLQSGLRK-Dabs, the K_m is 404 μM and the k_{cat} is 1.08 min^{-1} [26], quite similar to the numbers we obtained with the Rhodamine-based substrate. With Abz-TSAVLQSGFRK-DNP, the K_m is 253 μM and the k_{cat} is 0.3 min^{-1} [29]. The FRET substrates not only contain the P1 and P1′ amino acids, but, they also contain 5 amino acids before and after the cleavage site; thus, those substrates should occupy almost all of the specificity pockets in the enzyme. Although the Rhodamine-based substrates do not contain amino acids on the C-terminal side of the cleavage site and hence do not occupy those specificity pockets, this apparently does not matter in terms of kinetic constants that can be obtained.

The experiments to optimize assay conditions revealed several interesting characteristics of the SARS CoV main proteinase. The data points in the experiment in Fig. 4A where enzyme activity was plotted as a function of pH could best be fit to a model system with two ionizable groups, pK_a values of 6.8 and 8.7, and an optimal pH of 8. With the archetype cysteine proteinase papain, k_{cat}/K_m values as a function of pH exhibit a bell-shaped curve with a pH optimum of 6–7 and pK_a values of 3.3 for Cys25, and 8.3 for His159 [31]. On the other hand, the structure of the rhinovirus 2A proteinase [32] which is structurally similar to the SARS CoV main proteinase [5,33] also exhibits a bell-shaped k_{cat}/K_m versus pH curve but with an optimum pH of 8 and pK_a values of 7.34 for Cys106 and 8.54 for His28 [34]. The activity of the SARS CoV main proteinase was unusually insensitive to temperature. The optimal temperature was about 42 °C, but enzyme activity only increased by 37% between 25 and 37 °C. In contrast, the adenovirus proteinase which is also a cysteine proteinase has a temperature optimum of 45 °C, and enzyme activity increases 4-fold between 25 and 37 °C [11]. The SARS CoV main proteinase activity was very sensitive to ionic strength in that 80% of enzyme activity is lost by the presence of 100 mM NaCl. In contrast, the activity of the adenovirus proteinase in the absence of a nucleic acid cofactor is very insensitive to ionic strength. It has been postulated that there may be a salt bridge between Glu166 in the SARS CoV main proteinase and the P3 amino acid in the substrate if it is positively charged [25]. Perhaps this is why enzyme activity is so sensitive to ionic strength.

The assay described here for the SARS CoV main proteinase is extremely sensitive. To show exactly how sensitive the assay is, one must know the concentration of active enzyme. The crystal structure of the 3C-like proteinase from transmissible gastroenteritis virus [33] and from human coronavirus [5] is that of a dimer. And evidence has been published that indicates the dimer is the functional form of the enzyme [18,23,35]. We have characterized the monomer–dimer equilibrium of the SARS CoV main proteinase by small-angle X-ray scattering, chemical cross linking, and enzyme kinetics and determined that the equilibrium dissociation constant is 6.8 μM (Graziano et al., manuscript in preparation). This number was used to calculate the dimer concentration in Fig. 6. The substrate concentration in the experiment in Fig. 6 was 20 μM; since the K_m was 306 μM, the results of this experiment imply that if one were to assay the SARS CoV main proteinase at a substrate concentration equal to the K_m, enzyme activity from as low a concentration as 66 pM SARS CoV main proteinase dimer could be quantitatively observed.

The search for inhibitors of the SARS CoV main proteinase that may act as antiviral agents should be facilitated by use of this assay. The assay is particularly adaptable to high throughput screening. Very small microwells can be used to conserve enzyme, substrate and potential inhibitors. The assay is versatile in that substrate hydrolysis can be measured not only by fluorescence at 523 nm but also by absorbance at 496 nm. Kinetic analysis of compounds that inhibit the SARS CoV main proteinase can be designed to reveal whether a compound inhibits substrate binding or dimer formation. Finally, since some Rhodamine-based substrates have been shown to enter cells, $(Ala\text{-}Arg\text{-}Leu\text{-}Gln\text{-}NH)_2$-Rhodamine may be useful as a reporter for SARS coronavirus-infected cells.

Acknowledgements: Research supported by the Office of Biological and Environmental Research of the US Department of Energy under Prime Contract No. DE-AC0298CH10886 with Brookhaven National Laboratory, and by National Institutes of Health Grants AI41599 (W.F.M.) and AI056480 (J.J.D.). A.M.D. was supported by the Department of Energy's Office of Science Education and Technical Information, as a Science and Engineering Research Semester Program participant. We thank Dr. William Bellini from the Centers for Disease Control and Prevention for an extract from SARS coronavirus-infected cells that was used to clone the gene for the SARS CoV main proteinase and Lester C. Hart for help in preparing the manuscript.

Appendix A. Supplementary data

Supplementary data associated with this article can be found, in the online version, at doi:10.1016/j.febslet.2006.04.004.

References

[1] Drosten, C. et al. (2003) Identification of a novel coronavirus in patients with severe acute respiratory syndrome. N. Engl. J. Med. 348, 1967–1976.
[2] Ksiazek, T.G. et al. (2003) A novel coronavirus associated with severe acute respiratory syndrome. N. Engl. J. Med. 348, 1953–1966.
[3] Rota, P.A. et al. (2003) Characterization of a novel coronavirus associated with severe acute respiratory syndrome. Science 300, 1394–1399.
[4] Marra, M.A. et al. (2003) The Genome sequence of the SARS-associated coronavirus. Science 300, 1399–1404.
[5] Anand, K., Ziebuhr, J., Wadhwani, P., Mesters, J.R. and Hilgenfeld, R. (2003) Coronavirus main proteinase (3CLpro) structure: basis for design of anti-SARS drugs. Science 300, 1763–1767.
[6] Kim, J.C., Spence, R.A., Currier, P.F., Lu, X. and Denison, M.R. (1995) Coronavirus protein processing and RNA synthesis is inhibited by the cysteine proteinase inhibitor E64d. Virology 208, 1–8.
[7] Leytus, S.P., Melhado, L.L. and Mangel, W.F. (1983) Rhodamine-based compounds as fluorogenic substrates for serine proteases. Biochem. J. 209, 299–307.
[8] Leytus, S.P., Patterson, W.L. and Mangel, W.F. (1983) New class of sensitive, specific, and selective substrates for serine proteinases: fluorogenic, amino acid peptide derivatives of Rhodamine. Biochem. J. 215, 253–260.
[9] Leytus, S.P., Toledo, D.L. and Mangel, W.F. (1984) Theory and experimental method for determining individual kinetic constants for fast-acting, irreversible, protease inhibitors. Biochim. Biophys. Acta 788, 74–86.
[10] Mangel, W.F., McGrath, W.J., Toledo, D.L. and Anderson, C.W. (1993) Viral DNA and a viral peptide can act as cofactors of adenovirus virion proteinase activity. Nature 361, 274–275.
[11] McGrath, W.J., Abola, A.P., Toledo, D.L., Brown, M.T. and Mangel, W.F. (1996) Characterization of human adenovirus proteinase activity in disrupted virus particles. Virology 217, 131–138.
[12] Liu, J., Bhalgat, M., Zhang, C., Diwu, Z., Hoyland, B. and Klaubert, D.H. (1999) Fluorescent molecular probes V: a sensitive caspase-3 substrate for fluorometric assays. Bioorg. Med. Chem. Lett. 9, 3231–3236.
[13] Grant, S.K., Sklar, J.G. and Cummings, R.T. (2002) Development of novel assays for proteolytic enzymes using rhodamine-based fluorogenic substrates. J. Biomol. Screen. 7, 531–540.
[14] Lorey, S., Faust, J., Mrestani-Klaus, C., Kahne, T., Ansorge, S., Neubert, K. and Buhling, F. (2002) Transcellular proteolysis demonstrated by novel cell surface-associated substrates of dipeptidyl peptidase IV (CD26). J. Biol. Chem. 277, 33170–33177.
[15] Claveau, D., Riendeau, D. and Mancini, J.A. (2000) Expression, maturation, and rhodamine-based fluorescence assay of human cathepsin K expressed in CHO cells. Biochem. Pharmacol. 60, 759–769.
[16] Johnson, A.F., Struthers, M.D., Pierson, K.B., Mangel, W.F. and Smith, L.M. (1993) Nonisotopic DNA detection system employing elastase and fluorogenic rhodamine substrate. Anal. Biochem. 65, 2352–2359.
[17] Hegyi, A. and Ziebuhr, J. (2002) Conservation of substrate specificities among coronavirus main proteases. J. Gen. Virol. 83, 595–599.
[18] Fan, K. et al. (2004) Biosynthesis, purification and substrate specificity of servere acute respiratory syndrome coronavirus 3C-like proteinase. J. Biol. Chem. 279, 1637–1642.
[19] Snijder, E.J. et al. (2003) Unique and conserved features of genome and proteome of SARS-coronavirus, an early split-off from the coronavirus group 2 lineage. J. Mol. Biol. 331, 991–1004.
[20] Studier, F.W. (2005) Protein production by auto-induction in high-density shaking cultures. Protein Expr. Purif. 41, 207–234.
[21] Ziebuhr, J., Heusipp, G. and Siddell, S.G. (1997) Biosynthesis, purification, and characterization of the human coronavirus 229E 3C-like proteinase. J. Virol. 71, 3992–3997.
[22] Huang, C., Wei, P., Fan, K., Liu, Y. and Lai, L. (2004) 3C-like proteinase from SARS coronavirus catalyzes substrate hydrolysis by a general base mechanism. Biochemistry 43, 4568–4574.
[23] Kuo, C.J., Chi, Y.H., Hsu, J.T. and Liang, P.H. (2004) Characterization of SARS main protease and inhibitor assay using a fluorogenic substrate. Biochem. Biophys. Res. Commun. 318, 862–867.
[24] Li, M., Reddy, L.G., Bennett, R., Silva Jr., N.D., Jones, L.R. and Thomas, D.D. (1999) A fluorescence energy transfer method for analyzing protein oligomeric structure: application to phospholamban. Biophys. J. 76, 2587–2599.
[25] Fan, K., Ma, L., Han, X., Liang, H., Wei, P., Liu, Y. and Lai, L. (2005) The substrate specificity of SARS coronavirus 3C-like proteinase. Biochem. Biophys. Res. Commun. 329, 934–940.
[26] Chen, S. et al. (2005) Enzymatic activity characterization of SARS coronavirus 3C-like protease by fluorescence resonance energy transfer technique. Acta Pharmacol. Sin. 26, 99–106.
[27] Chou, C.Y., Chang, H.C., Hsu, W.C., Lin, T.Z., Lin, C.H. and Chang, G.G. (2004) Quaternary structure of the severe acute respiratory syndrome (SARS) coronavirus main protease. Biochemistry 43, 14958–14970.
[28] Hsu, J.T. et al. (2004) Evaluation of metal-conjugated compounds as inhibitors of 3CL protease of SARS-CoV. FEBS Lett. 574, 116–120.
[29] Kuang, W.F., Chow, L.P., Wu, M.H. and Hwang, L.H. (2005) Mutational and inhibitive analysis of SARS coronavirus 3C-like protease by fluorescence resonance energy transfer-based assays. Biochem. Biophys. Res. Commun. 331, 1554–1559.
[30] Liu, Y.C., Huang, V., Chao, T.C., Hsiao, C.D., Lin, A., Chang, M.F. and Chow, L.P. (2005) Screening of drugs by FRET analysis identifies inhibitors of SARS-CoV 3CL protease. Biochem. Biophys. Res. Commun. 333, 194–199.
[31] Dardenne, L.E., Werneck, A.S., Neto, M.D.O. and Bisch, P.M. (2003) Electrostatic properties in the catalytic site of papain: a possible regulatory mechanism for the reactivity of the ion pair. Proteins Struct. Funct. Genet. 52, 236–253.
[32] Petersen, J.F.W., Cherney, M.M., Liebig, H.-D., Skern, T., Kuechler, E. and James, M.N.G. (1999) The structure of the 2A proteinase from a common cold virus: a proteinase responsible for the shut-off of host-cell protein synthesis. EMBO J. 18, 5463–5475.
[33] Anand, K., Palm, G.J., Mesters, J.R., Siddell, S.G., Ziebuhr, J. and Hilgenfeld, R. (2002) Structure of coronavirus main proteinase reveals combination of a chymotrpsin fold with an extra α-helical domain. EMBO J. 21, 3213–3224.
[34] Sarkany, Z., Skern, T. and Polgar, L. (2000) Characterization of the active site thiol group of the rhinovirus 2A proteinase. FEBS Lett. 481, 289–292.
[35] Shi, J.H., Wei, Z. and Song, J.X. (2004) Dissection study on the SARS 3C-like protease reveals the critical role of the extra domain in dimerization of the enzyme: defining the extra domain as a new target for design of highly-specific protease inhibitors. J. Biol. Chem. 279, 24765–24773.